Thermal Conductivity Evidence for a $d_{x^2-y^2}$ Pairing Symmetry in the Heavy-Fermion $CeIrIn_5$ Superconductor

Y. Kasahara,[1] T. Iwasawa,[1] Y. Shimizu,[1] H. Shishido,[1] T. Shibauchi,[1] I. Vekhter,[2] and Y. Matsuda[1,3]

[1]*Department of Physics, Kyoto University, Kyoto 606-8502, Japan*

[2]*Department of Physics and Astronomy, Louisiana State University, Baton Rouge, Louisiana, 70803, USA*

[3]*Institute for Solid State Physics, University of Tokyo, Kashiwanoha, Kashiwa, Chiba 277-8581, Japan*

(Received 30 November 2007; published 20 May 2008)

The phase diagram of the quasi-2D Ce(Ir, Rh)In_5 system contains two distinct superconducting domes. By the thermal transport measurements in rotating magnetic fields $\boldsymbol{H}$, we pinned down the superconducting gap structure of $CeIrIn_5$ in the second dome, located distant from the first dome in proximity to an antiferromagnetic quantum critical point. Clear fourfold oscillation was observed when $\boldsymbol{H}$ is rotated within the ab plane, while no oscillation was observed within the bc plane. In sharp contrast to previous reports, our results are most consistent with $d_{x^2-y^2}$ symmetry, implying that the superconductivity in the second phase is also mediated by antiferromagnetic spin fluctuations.

DOI: 10.1103/PhysRevLett.100.207003 PACS numbers: 74.20.Rp, 74.25.Dw, 74.25.Fy, 74.70.Tx

The relationship between the magnetism and unconventional superconductivity, whereby the gap function $\Delta(\boldsymbol{k})$ has nodes on the Fermi surface where $\Delta(\boldsymbol{k}) = 0$, in heavy-fermion (HF) compounds continues to be a central focus of investigations into strongly correlated electron systems [1]. Many analyses have focused on the superconductivity mediated by magnetic fluctuations, often in proximity to a quantum critical point (QCP), where the magnetic ordering temperature is driven to zero by an external parameter such as pressure or chemical substitution. Indeed, unconventional superconductivity appears in the vicinity of an antiferromagnetic (AF) QCP in most Ce-based HF compounds, including $CeIn_3$, $CePd_2Si_2$ [2], $CeCoIn_5$, [3] and $CeRhIn_5$ [4], as well as high-T_c cuprates.

Notable counterexamples have been recently reported in two Ce compounds, where two distinct domes of different HF superconducting phases appear as a function of pressure or chemical substitution. The first example is $CeCu_2Si_2$, with one superconducting dome at low pressure around the AF QCP, and another dome emerging at high pressure distant from the QCP [5]. The superconductivity in the low pressure dome is consistent with the magnetically mediated pairing, while Cooper pairing glued by the Ce-valence fluctuations was proposed for the high pressure region with no discernible AF fluctuations [5,6].

The second example is a quasi-2D $CeIrIn_5$ ($T_c = 0.4$ K) [3], whose phase diagram is shown in the inset of Fig. 1 [7,8]. In this system the Rh substitution for Ir acts as a negative chemical pressure that increases AF correlations. In $CeRh_{1-x}Ir_xIn_5$, the ground state continuously evolves from AF metal (AFM) ($x < 0.5$) to superconductor ($x > 0.5$). T_c shows a maximum at $x \sim 0.7$ and a cusplike minimum at $x \sim 0.9$, forming the first dome (SC1). In $CeIrIn_5$ ($x = 1$), T_c increases with pressure and exhibits a maximum ($T_c = 1$ K) at $P \sim 3$ GPa, forming a second dome (SC2). The strong AF fluctuations associated with the AF QCP nearby are observed in SC1 [8,9], but are strongly suppressed with pressure, in SC2, away from the AF QCP [8–10]. Moreover, the nature of the AF fluctuations in magnetic fields in $CeIrIn_5$ is very different from that in $CeCoIn_5$ and AF $CeRhIn_5$ [11–13]. Thus superconductivity in $CeIrIn_5$ at ambient pressure may be distinct from that in $CeCoIn_5$ and $CeRhIn_5$, although all three compounds share similar band structure [14].

Hence a major outstanding question is the nature of the pairing interaction in $CeIrIn_5$. By analogy with $CeCu_2Si_2$, $CeIrIn_5$ in SC2 was suggested to be a strong candidate for

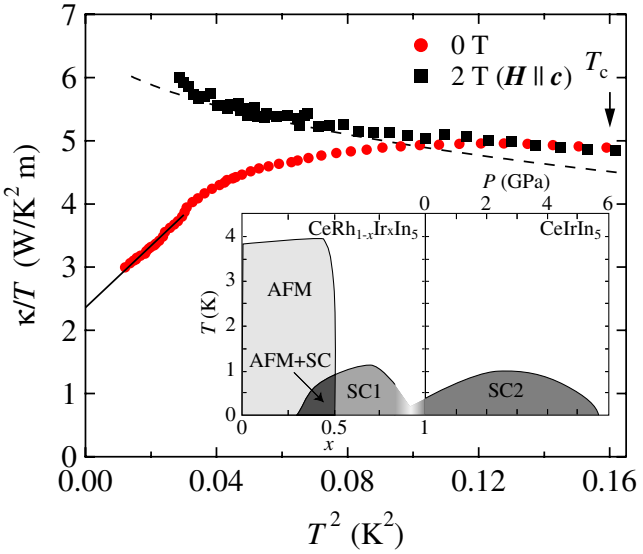

FIG. 1 (color online). Temperature dependence of κ/T as a function of T^2 in zero field and above H_{c2}^c ($H = 2$ T). The solid line represents $\kappa/T = \kappa_{00}/T + AT^2$; the dashed line shows κ/T obtained from the resistivity using the Wiedemann-Franz law. Inset: phase diagram of Ce(Ir, Rh)In_5 as a function of Ir concentration and pressure, from Refs. [7,8].

the Ce-valence fluctuation mediated superconductor [6]. To elucidate the pairing symmetry, identification of the superconducting gap structure is of primary importance. Measurements of nuclear quadrupole resonance [9,10], thermal conductivity κ [15,16], and heat capacity [15] revealed that the superconductivity of $CeIrIn_5$ is unconventional, with line nodes in the gap. Very recently, the interplane and intraplane thermal conductivity in zero field have been reported to have a large residual anisotropy in $CeIrIn_5$ [16], in contrast to the small anisotropy in $CeCoIn_5$ [17]. From these results, the gap function of $CeIrIn_5$ was suggested to be of hybrid type, $k_z(k_x + ik_y)$, or E_g symmetry [16], similar to UPt_3 [18], and in sharp contrast to the $d_{x^2-y^2}$ gap in $CeCoIn_5$ (and most likely in $CeRhIn_5$ under pressure) [19]. However, as pointed out in Ref. [20], the anisotropy of κ alone is not sufficient to establish the hybrid gap, and further experiments aimed at clarifying the shape of the superconducting gap are needed.

Here, to shed light on the pairing mechanism of $CeIrIn_5$, we measured the thermal conductivity in a magnetic field $\boldsymbol{H}$ rotated relative to the crystal axes. We provide strong evidence of $d_{x^2-y^2}$ gap symmetry. The results put a constraint on the pairing mechanism in $CeIrIn_5$.

Single crystals were grown by the self-flux method. The bulk transition temperature is 0.4 K, and upper critical fields parallel to the ab plane and the c axis, H_{c2}^{ab} and H_{c2}^{c}, are 1.0 T and 0.5 T at $T = 0$ K, respectively. We measured the thermal conductivity κ along the tetragonal a axis (heat current $\boldsymbol{q} \parallel a$) on the sample with a rectangular shape ($2.8 \times 0.45 \times 0.10$ mm^3). To apply $\boldsymbol{H}$ with high accuracy (misalignment of less than 0.05°) relative to the crystal axes, we used a system with two superconducting magnets generating $\boldsymbol{H}$ in two mutually orthogonal directions and a dilution refrigerator equipped on a mechanical rotating stage at the top of the Dewar.

Figure 1 shows κ/T as a function of T^2 at $H = 0$ and above H_{c2}^{c}. The overall behavior of κ/T is similar to those reported in Refs. [15,16]. In zero field, κ/T decreases with decreasing T after showing a broad maximum at T_c, similar to UPt_3 [21] and $CePt_3Si$ [22]. The value of κ/T at T_c is nearly 30% smaller than that reported in Ref. [16] and nearly 3 times larger than that reported in Ref. [15]. The dashed line is κ/T obtained from the Wiedemann-Franz law, $\kappa/T = L_0/\rho$, where $L_0 = \frac{\pi^2}{3}(\frac{k_B}{e})^2$ and ρ is the normal state resistivity. The observed κ/T is close to L_0/ρ, indicating the dominant electronic contribution in the heat transport [23].

First, let us consider the thermal conductivity at $H = 0$. As shown in Fig. 1, κ/T at low T is well fitted by $\kappa/T = \kappa_{00}/T + AT^2$, with the clearly resolved residual term κ_{00}/Tas $T \to 0$ K. This indicates the existence of a residual normal fluid, expected for nodal superconductors with impurities. For a gap with line nodes, the magnitude of κ_{00}/T is independent of impurity concentration [24]. Our value of $\kappa_{00}/T = 2.3 \pm 0.2$ W/K^2 m agrees, within error bars, with that reported in Ref. [16] ($\kappa_{00}/T = 2.1 \pm 0.2$ W/K^2 m) and is consistent with the theoretical estimate for a superconductor with line node.

The next question is the nodal topology. Thermal conductivity is a powerful directional probe of the nodal structure: Recent measurements of both κ and the heat capacity with $\boldsymbol{H}$ applied at varying orientation relative to the crystal axes established the superconducting gap structure in several systems [19,25,26]. In nodal superconductors the heat transport is dominated by delocalized near-nodal quasiparticles (QPs). The applied field creates a circulating supercurrent flow $\boldsymbol{v}_s(\boldsymbol{r})$ associated with vortices. The Doppler shift of the energy of a quasiparticle with momentum $\boldsymbol{p}$, $E(\boldsymbol{p}) \to E(\boldsymbol{p}) - \boldsymbol{v}_s \cdot \boldsymbol{p}$, is important near the nodes, where the local energy gap is small, $\Delta(\hat{\boldsymbol{p}}) < |\boldsymbol{v}_s \cdot \boldsymbol{p}|$. Consequently the density of states (DOS) depends sensitively on the angle between $\boldsymbol{H}$ and the nodal directions [27]. Clear twofold or fourfold oscillations of thermal conductivity and heat capacity due to nodes have been observed in UPd_2Al_3 [28], $YBa_2Cu_3O_7$ [29], $CeCoIn_5$ [26,30], and κ-$(BEDT\text{-}TTF)_2Cu(NCS)_2$ [31] when $\boldsymbol{H}$ is rotated relative to the crystal axes.

Figures 2(a) and 2(b) show the angular variation of the thermal conductivity at 200 mK ($k_BT/\Delta \sim 0.2$) as $\boldsymbol{H}$ is rotated within the bc plane at $|\boldsymbol{H}| = 0.05$ T [$H/H_{c2}^{c}(T) \simeq 0.14$] and at $|\boldsymbol{H}| = 0.1$ T [$H/H_{c2}^{ab}(T) \simeq 0.14$], and within the 2D ab plane at $|\boldsymbol{H}| = 0.1$ T [$H/H_{c2}^{ab}(T) \simeq 0.14$], respectively. Here $\theta = (\boldsymbol{H}, c)$ and $\phi = (\boldsymbol{H}, a)$ are the polar and azimuthal angles, respectively. For the field rotated

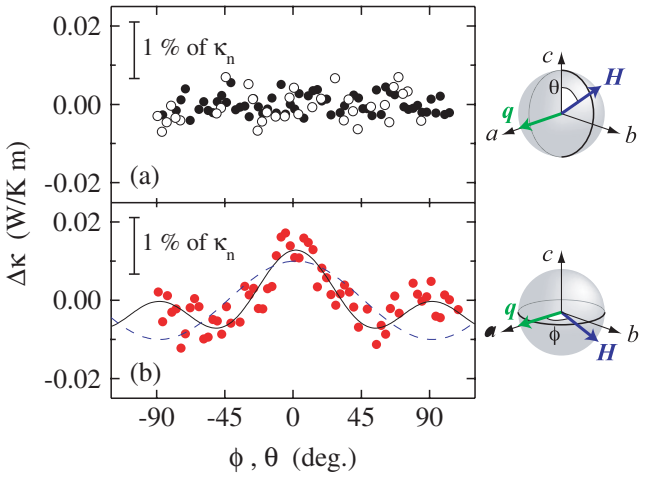

FIG. 2 (color online). Angular variation of the thermal conductivity $\Delta\kappa \equiv \kappa - \kappa_0$at $T = 200$ mK with rotating $\boldsymbol{H}$ (a) within the bc plane as a function of polar angle θ for $|\boldsymbol{H}| = 0.05$ T (filled circles) and 0.10 T (open circles) and (b) within the 2D ab plane as a function of azimuthal angle ϕ for $|\boldsymbol{H}| = 0.10$ T. Here κ_0 is the angular average of κ. The thermal current $\boldsymbol{q}$ is applied parallel to the a axis. The dashed line shows the twofold ($\cos 2\phi$) variation. The solid line is the fit by $\kappa(\phi) = \kappa_0 + C_{2\phi}\cos 2\phi + C_{4\phi}\cos 4\phi$, where $C_{2\phi}$, and $C_{4\phi}$ are constants.

within the ab plane ($\theta = 90°$) $\kappa(\phi)$ exhibits a distinct oscillation as a function of ϕ, which is characterized by peaks at $\phi = 0°$ and $\pm 90°$ and minima at around $\pm 45°$. As shown by the solid line, $\kappa(\phi)$ can be decomposed into three terms, $\kappa(\phi) = \kappa_0 + \kappa_{2\phi} + \kappa_{4\phi}$, where $\kappa_{2\phi} = C_{2\phi} \cos 2\phi$ and $\kappa_{4\phi} = C_{4\phi} \cos 4\phi$ have the two- and fourfold symmetry with respect to ϕ, respectively. We note that, as shown by the dashed line, $\kappa(\phi)$ with minima at $\pm 45°$ and peaks at $\pm 90°$ cannot be fitted only by the $\kappa_{2\phi}$ term, indicating the presence of the fourfold term. In sharp contrast to $\boldsymbol{H}$ rotating within the ab plane, no oscillation is observed when rotating $\boldsymbol{H}$ within the bc plane; the amplitude of the oscillation is less than 0.2% (0.3%) of κ_n for $|\boldsymbol{H}| = 0.05$ T (0.1 T) if it exists, where κ_n is the normal state thermal conductivity measured above H_{c2}. The $\kappa_{2\phi}$ term arises from the difference between transport parallel and perpendicular to the vortices. Since for $\boldsymbol{H}$ within the bc plane the field is always normal to $\boldsymbol{q}$, the $\kappa_{2\phi}$ term is absent for this geometry.

We address the origin of the fourfold oscillation. Figures 3(a)–3(d) display $\kappa_{4\phi}$ normalized by κ_n at 200 mK below $H_{c2}^{ab}(T)$ ($\simeq$0.7 T). In the normal state above H_{c2}^{ab}, no discernible oscillation was observed (not shown). At 0.69 T just below $H_{c2}^{ab}(T)$, $\kappa_{4\phi}$ exhibits a minimum at $\phi = 0°$ ($C_{4\phi} < 0$). At $H = 0.5$ T, $\kappa_{4\phi}$ oscillation vanishes. Further decrease of H leads to the appearance of distinct $\kappa_{4\phi}$ oscillation with a maximum at $\phi = 0°$ ($C_{4\phi} > 0$) at $H = 0.1$ and 0.25 T. Figure 3(e) shows the H dependence of $C_{4\phi}/\kappa_n$. Fourfold oscillation may originate from (i) the nodal structure and (ii) in-plane anisotropy of the Fermi surface and H_{c2}^{ab}. It should be stressed that the sign of $C_{4\phi}$ just below H_{c2}^{ab} is the same as that expected from the in-plane anisotropy of H_{c2}^{ab} [$H_{c2} \parallel (100) > H_{c2} \parallel (110)$] [32], whereas its sign at low fields is opposite. This immediately indicates that the origin of the fourfold symmetry at low fields is not due to the anisotropy of the Fermi surface or H_{c2}^{ab}. A rough estimate of the amplitude of the fourfold term in layered d wave superconductors yields $C_{4\phi}/\kappa_n = 0.082 \frac{v_F v_F' eH}{3\pi\Gamma\Delta} \ln(\sqrt{32\Delta/\pi\hbar\Gamma})$, where Δ is the superconducting gap, Γ is the QP relaxation rate, v_F and v_F' are the in-plane and out-of-plane Fermi velocities [33]. Using $\Gamma \sim 1.3 \times 10^{11}$ s^{-1}, $2\Delta/k_B T_c \sim 5$, $v_F \sim 1 \times 10^4$ m/s, and $v_F' \sim 5 \times 10^3$ m/s [9,30] gives $C_{4\phi}/\kappa_n \sim 2\%$, of the same order as the data. These results lead us to conclude that the fourfold symmetry at low fields originates from the nodal structure.

The distinct fourfold oscillation within the ab plane, together with the absence of the oscillation within the bc plane, definitely indicates the vertical line nodes perpendicular to the ab plane, and excludes a horizontal line of nodes at least in the dominant heavy electron bands. Recall that in UPd_2Al_3 with horizontal line node, clear oscillations of $\kappa(\theta)$ are observed when rotating $\boldsymbol{H}$ within the ac plane [28]. One could argue that the absence of oscillations within the bc plane shown in Fig. 2(a) is due to relatively high temperature ($k_B T/\Delta \sim 0.2$), but the simultaneous observation of the fourfold oscillation within the ab plane at the same T rules out such a possibility.

Thus the superconducting symmetry of $CeIrIn_5$ is narrowed down to either $d_{x^2-y^2}$ or d_{xy}. Further identification relies on the evolution of the oscillations with temperature

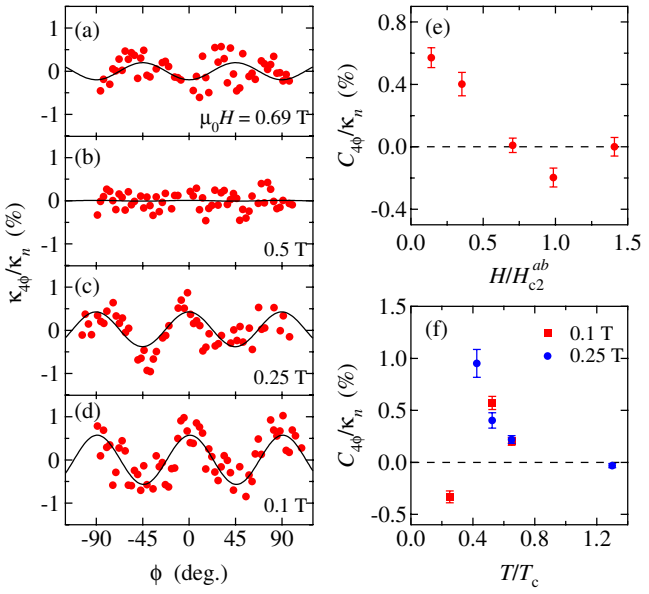

FIG. 3 (color online). (a)–(d) The fourfold component $\kappa_{4\phi}$normalized by κ_n with $\boldsymbol{H}$ rotated in the ab plane at $T =$ 200 mK at $|\boldsymbol{H}| = 0.69$, 0.5, 0.25, and 0.1 T, respectively. The upper critical field is $H_{c2}^{ab} \gtrsim 0.7$ T at this temperature. The solid lines represent the fit by $C_{4\phi} \cos 4\phi$. (e) $C_{4\phi}/\kappa_n$ at $T = 200$ mK as a function of H/H_{c2}^{ab}. (f) $C_{4\phi}/\kappa_n$ at $H = 0.1$ and 0.25 T as a function of T/T_c.

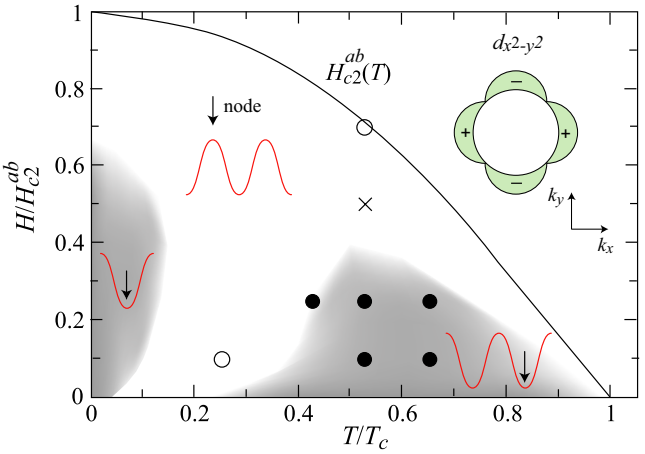

FIG. 4 (color online). H-T phase diagram for the fourfold term $\kappa_{4\phi}$ in $\boldsymbol{H}$ rotated within the ab plane. Solid (open) circles indicate points with maxima (minima) of $\kappa_{4\phi}$ at $\phi = 0°$. The shaded (unshaded) regions correspond to minima (maxima) of $\kappa_{4\phi}$ for $\boldsymbol{H}$ along the nodal directions [35].

and field. In the low-T, low-H limit, the Doppler shifted DOS shows a maximum (minimum) when $\boldsymbol{H}$ is along the antinodal (nodal) directions. However, according to recent microscopic calculations, the pattern is inverted at higher T, H due to vortex scattering, and the fourfold components of the specific heat and of the thermal conductivity have similar behavior across the phase diagram [34,35]. In Fig. 3(f) we plot $C_{4\phi}/\kappa_n$ as a function of temperature. At $H = 0.1$ T, the sign change indeed occurs at $T/T_c \simeq 0.25$. Figure 4 displays the H-T phase diagram for the fourfold component. The solid (open) circles represent the points at which observed $\kappa_{4\phi}$ exhibits a maximum (minimum) at $\phi = 0°$, and the shading indicates the calculated anisotropy of the thermal conductivity for a d-wave superconductor from Ref. [35]. The shaded (unshaded) regions correspond to the region where $\kappa_{4\phi}$ has a minimum (maximum) for the field in the nodal direction. The calculation is for a corrugated cylindrical Fermi surface, similar to that of the main Fermi surface sheet of $CeIrIn_5$, and the results well reproduce the observed sign change of $\kappa_{4\phi}$. Ref. [20] showed that small deviations from cylindrical symmetry are sufficient to reconcile the vertical lines of nodes with the results of Ref. [16]. We assume that these small deviations weakly affect the phase diagram of Fig. 4. Since the minimum (maximum) of $\kappa_{4\phi}$ occurs at $\phi = 45°$ inside (outside) the shaded region, the nodes are located at $\pm 45°$. We thus conclude that the gap symmetry of $CeIrIn_5$ is $d_{x^2-y^2}$.

The $d_{x^2-y^2}$ symmetry implies that the superconductivity is most likely to be mediated by the AF spin fluctuations, not by the Ce-valence fluctuations [36]. Our result is also at odds with the hybrid gap function with horizontal node proposed in Ref. [16]. Recent study of $CeCo(In_{1-x}Cd_x)_5$ revealed that the superconductivity in $CeCoIn_5$ occurs in the proximity to the AF ordered phase [37]. Therefore it is natural to consider that the symmetry of the SC1 phase is $d_{x^2-y^2}$, the same as $CeCoIn_5$ [19]. It is then intriguing that the superconductivity in the SC1 and SC2 phases has the same gap symmetry.

In conclusion, the measurements of the thermal conductivity under rotated magnetic fields provide strong evidence that the superconducting gap of $CeIrIn_5$ at ambient pressure has vertical line nodes, and is of $d_{x^2-y^2}$ symmetry. This indicates that two distinct domes of HF superconducting phases possess the same superconducting symmetry, in which AF fluctuations appear to play an important role. The determined gap symmetry in $CeIrIn_5$ which is located in the second superconducting phase, further restricts theories of the pairing mechanism.

We thank H. Ikeda, K. Kontani, P. Thalmeier, and S. Watanabe for helpful discussions.

[1] P. Thalmeier and G. Zwicknagl, in *Handbook on the Physics and Chemistry of Rare Earths* (North Holland, Amsterdam, 2005), Vol. 34.
[2] N. D. Mathur *et al.*, Nature (London) **394**, 39 (1998).
[3] C. Petrovic *et al.*, J. Phys. Condens. Matter **13**, L337 (2001).
[4] H. Hegger *et al.*, Phys. Rev. Lett. **84**, 4986 (2000).
[5] H. Q. Yuan *et al.*, Science **302**, 2104 (2003).
[6] A. T. Holmes, D. Jaccard, and K. Miyake, J. Phys. Soc. Jpn. **76**, 051002 (2007).
[7] M. Nicklas *et al.*, Phys. Rev. B **70**, 020505(R) (2004).
[8] S. Kawasaki *et al.*, Phys. Rev. Lett. **96**, 147001 (2006).
[9] S. Kawasaki *et al.*, Phys. Rev. Lett. **94**, 037007 (2005).
[10] G.-q. Zheng *et al.*, Phys. Rev. Lett. **86**, 4664 (2001).
[11] J. Paglione *et al.*, Phys. Rev. Lett. **91**, 246405 (2003); A. Bianchi *et al.*, Phys. Rev. Lett. **91**, 257001 (2003); T. Park *et al.*, Nature (London) **440**, 65 (2006).
[12] C. Capan *et al.*, Phys. Rev. B **70**, 180502 (2004).
[13] S. Nair *et al.*, arXiv:0710.5011.
[14] R. Settai, T. Takeuchi, and Y. Onuki, J. Phys. Soc. Jpn. **76**, 051003 (2007); Y. Haga *et al.*, Phys. Rev. B **63**, 060503(R) (2001).
[15] R. Movshovich *et al.*, Phys. Rev. Lett. **86**, 5152 (2001).
[16] H. Shakeripour *et al.*, Phys. Rev. Lett. **99**, 187004 (2007).
[17] M. A. Tanatar *et al.*, Phys. Rev. Lett. **95**, 067002 (2005).
[18] B. Lussier, B. Ellman, and L. Taillefer, Phys. Rev. Lett. **73**, 3294 (1994).
[19] For a review, see Y. Matsuda, K. Izawa, and I. Vekhter, J. Phys. Condens. Matter **18**, R705 (2006).
[20] I. Vekhter and A. Vorontsov, Phys. Rev. B **75**, 094512 (2007).
[21] H. Suderow *et al.*, Phys. Rev. Lett. **80**, 165 (1998).
[22] K. Izawa *et al.*, Phys. Rev. Lett. **94**, 197002 (2005).
[23] Normal state κ/T slightly above L_0/ρ suggests a small phonon contribution to κ, about an order of magnitude smaller than the electronic contribution at T_c.
[24] L. Taillefer *et al.*, Phys. Rev. Lett. **79**, 483 (1997).
[25] T. Park and M. B. Salamon, Mod. Phys. Lett. B **18**, 1205 (2004).
[26] T. Sakakibara *et al.*, J. Phys. Soc. Jpn. **76**, 051004 (2007).
[27] I. Vekhter *et al.*, Phys. Rev. B **59**, R9023 (1999).
[28] T. Watanabe *et al.*, Phys. Rev. B **70**, 184502 (2004).
[29] H. Aubin *et al.*, Phys. Rev. Lett. **78**, 2624 (1997).
[30] K. Izawa *et al.*, Phys. Rev. Lett. **87**, 057002 (2001).
[31] K. Izawa *et al.*, Phys. Rev. Lett. **88**, 027002 (2001).
[32] F. Weickert *et al.*, Phys. Rev. B **74**, 134511 (2006).
[33] H. Won and K. Maki, arXiv:cond-mat/0004105.
[34] A. Vorontsov and I. Vekhter, Phys. Rev. Lett. **96**, 237001 (2006).
[35] A. Vorontsov and I. Vekhter, Phys. Rev. B **75**, 224501 (2007); Phys. Rev. B **75**, 224502 (2007).
[36] For example, K. Tanaka *et al.*, J. Phys. Condens. Matter **19**, 406219 (2007).
[37] L. D. Pham *et al.*, Phys. Rev. Lett. **97**, 056404 (2006).